Constraining the black hole mass and accretion rate in the narrow-line Seyfert 1 RE J1034+396

E. M. Puchnarewicz and K. O. Mason
Mullard Space Science Laboratory, Holmbury St. Mary, Dorking, Surrey RH5 6NT, UK
emp@mssl.ucl.ac.uk, kom@mssl.ucl.ac.uk

A. Siemiginowska and A. Fruscione
Harvard-Smithsonian Center for Astrophysics, 60 Garden Street, MS-4, Cambridge MA 02138, USA
aneta@head-cfa.harvard.edu, antonell@head-cfa.harvard.edu

A. Comastri
Osservatorio Astronomico di Bologna, via Ranzani 1, I-40127 Bologna, Italy
comastri@astbo3.bo.astro.it

F. Fiore[1]
Osservatorio Astronomico di Roma, via Frascati 33, I-00040 Monteporzio (Rm), Italy
fiore@quasar.mporzio.astro.it
and

I. Cagnoni[1]
Scuola Internazionale Superiore di Studi Avanzati, via Beirut 2-4, 34014 Trieste, Italy
ilaria@head-cfa.harvard.edu

ABSTRACT

We present a comprehensive study of the spectrum of the narrow-line Seyfert 1 galaxy RE J1034+396, summarizing the information obtained from the optical to X-rays with observations from the William Herschel 4.2m Telescope (WHT), the Hubble Space Telescope (*HST*), the Extreme UltraViolet Explorer (*EUVE*), *ROSAT*, *ASCA* and *Beppo-SAX*. The *Beppo-SAX* spectra reveal a soft component which is well-represented by two blackbodies with $kT_{\rm eff}$=60 eV and 160 eV, mimicking that expected from a hot, optically-thick accretion disc around a low-mass black hole. This is borne out by our modeling of the optical to X-ray nuclear continuum, which constrains the physical parameters of a NLS1 for the first time. The models demonstrate that RE J1034+396 is likely to be a system with a nearly edge-on accretion disk (60 to 75° from the disk axis), accreting at nearly Eddington rates (0.3 to 0.7 $L_{\rm Edd}$) onto a low mass black hole (M_{bh} ~2 to 10×10^6 $M_\odot$). This is consistent with the hypothesis that NLS1s are Seyfert-scale analogies of Galactic Black Hole Candidates. The unusually high temperature of the big blue bump reveals a flat power-law like continuum in the optical/UV which is consistent with an extrapolation to the hard X-ray power-law, and which we speculate may be similar to the continuum component observed in BL Lac objects in their quiescent periods. From the *Beppo-SAX* and *ASCA* data, we find that the slope of the hard X-ray power-law depends very much on the form of the soft component which is assumed. For our best-fitting models, it lies somewhere between α=0.7 and 1.3 and thus may not be significantly softer than AGN in general.

Subject headings: accretion, accretion disks – galaxies: active – galaxies: nuclei – galaxies: Seyfert – X-rays: galaxies – galaxies: individual (RE J1034+396)

1. Introduction

The narrow-line Seyfert 1 (NLS1) type of AGN has proven to be a valuable and a fascinating resource for the study of the class as a whole. They have very strong soft X-ray excesses (Puchnarewicz et al. 1992; Boller, Brandt & Fink 1996), are often highly variable (Brandt, Fabian & Pounds 1996; Boller et al. 1997) and, in some cases, the optical/UV big blue bump (BBB) component is so hot that it is shifted into the UV/EUV regime, leaving a bare, power-law-like continuum component in the optical (Puchnarewicz et al. 1995).

One of the earliest hypotheses put forward to explain the strong and variable ultra-soft X-ray excesses, was a high mass accretion rate onto a relatively low-mass black hole (Pounds, Done & Osborne 1995). This was originally proposed for RE J1034+396, by analogy with the properties of Galactic Black Hole Candidates (GBHCs). An alternative model was that such systems were geometrically-thick accretion disks (ADs) viewed face-on, lying co-planar with a flattened broad line region [BLR; Puchnarewicz et al. (1992)].

In our initial study of RE J1034+396 (Puchnarewicz et al. 1995), we showed that the overall IR to X-ray spectrum compared well with the combination of a geometrically-thin, optically-thick AD and an underlying power-law with a slope, α=1.3 (α is defined throughout such that $F_\nu \propto \nu^{-\alpha}$). The Kerr black hole mass was 7×10^5 $M_\odot$, the accretion rate was 0.073 $M_\odot$ yr^{-1} and the disk was viewed at an angle of 60° from its axis. However, this was for illustrative purposes only and no constraints were placed on these parameters. Thus, while this might have suggested the presence of a low-mass black hole for RE J1034+396, consistent with the GBHC analogy, solutions at higher black hole mass could not be ruled out.

With the launch of *Beppo-SAX* and the inclusion of RE J1034+396 in the NLS1 core program, came the opportunity to place meaningful constraints on black hole mass (M_{bh}), accretion rate ($\dot{M}$) and inclination. RE J1034+396 was also due to be observed with *HST* within a few months of *Beppo-SAX*, and an optical spectrum was also scheduled in *WHT* service time within a few weeks. Thus a quasi-simultaneous spectrum, providing the most complete coverage possible from the optical to mid X-rays was available. Simultaneity is important for a NLS1 due to the variable nature of the class, although RE J1034+396, contrary to its counterparts, has shown remarkable stability. Thus these data have provided the best opportunity yet to fit AD models and provide constraints on the defining parameters of an NLS1. Using a combination of a power-law and an optically-thick, geometrically-thin Kerr AD model, we present fits to the observed spectrum of RE J1034+396, measuring M_{bh} and $\dot{M}$ and constraining the inclination for the first time, and discuss the results in the context of the GBHC model.

The improved UV and optical data presented here have also allowed us to re-visit the issue of what is producing the optical/UV continuum in this object. Our previous work had suggested a power-law-like continuum rising towards the red, which was not due to the host galaxy or the BBB. We have separated out the galaxy component from the spatially-resolved optical spectrum obtained and, when combined with the *HST* data, examined the pure nuclear component with a greater degree of clarity. The results and their implications for the production of the optical continuum in AGN are also discussed in this paper.

2. Data

RE J1034+396 has been observed on several occasions at different wavelengths from the radio to X-rays (Puchnarewicz et al. 1995; Pounds, Done & Osborne 1995; Puchnarewicz, Mason & Siemiginowska 1998; Breeveld & Puchnarewicz 1998). In this paper, we present data taken at optical, EUV (*EUVE*), soft X-ray (*ROSAT* HRI and *SAX* LECS) and medium X-ray (*SAX* LECS and MECS) energies which were taken quasi-simultaneously with the *HST*-FOS spectrum. We also analyze previously unreported *ROSAT* HRI (taken 1994 November 20) and *ASCA* data (taken 1995 May 18) to check for variability in this object.

2.1. Optical spectra

RE J1034+396 was observed on the night of 1996 March 24 using the twin-armed ISIS spec-

[1] Harvard-Smithsonian Center for Astrophysics, 60 Garden Street, MS-4, Cambridge MA 02138, USA

trograph on the William Herschel Telescope on La Palma as part of the service observing program (observers D. Pollacco and D. King). The input starlight was divided between the red and blue arms of the spectrograph by means of a dichroic filter whose crossover wavelength is 5400Å. The R316R grating was used in the red arm of the spectrograph, centered on a wavelength of 6677 Å. The blue arm utilized the R300B grating centered on 4519 Å. The red spectrum spanned the wavelength range 6000Å to 7700Å, while the blue spectrum extended from 3800Å to 5300Å. The data were recorded on TEK 1024 square CCDs. Two exposures, each of 600s duration, were taken of RE J1034+396 and the resulting images combined during analysis (eliminating cosmic ray events) to give a total effective exposure time of 1200s. The sky was clear throughout. Standard exposures of wavelength calibration arcs and flux calibration stars were made immediately following the RE J1034+396 observations using the same instrumental set-up.

The integrated spectrum of RE J1034+396 is clearly contaminated by light from the host galaxy, particularly in the red. The separate contributions of the active nucleus and the underlying galaxy are clearly evident in the cross-dispersion spatial profile. To remove the worst effects of the galaxy contamination on the nuclear spectrum, the 2-D image of the spectrum was divided into 25 Å bins and the mean spatial profile in the cross-dispersion direction formed for each bin. Two Gaussian profiles superimposed on a flat background were then fitted simultaneously to the spatial data in each bin, to model the nuclear and extended components respectively. Gaussian functions were found to be satisfactory and robust representations of the spatial data for the purposes of this decomposition. The flux in the two Gaussian components as a function of wavelength thus represents the spectrum of the nuclear and extended emission respectively.

2.2. *HST* observations

RE J1034+396 was observed by *HST* on 1997 January 31 using three gratings (G130L, G190L and G270L) covering the range 1100 Å to 3300 Å. Full details of the observations and data reduction were presented in Puchnarewicz, Mason & Siemiginowska (1998).

The *HST* spectrum was combined with the deconvolved optical nuclear spectrum and the resulting optical/UV continuum was fitted with a power-law model. The best fit was obtained for α=0.9, having removed obvious emission and absorption features before fitting. Errors are difficult to determine precisely, because the relative normalization of the two spectra is not known (the data were not taken simultaneously and different slit widths and positions were used) and because of the difficulty in securely removing absorption and emission features before fitting the continuum. Assuming, therefore, a conservative error of 20% on the optical and UV fluxes, gave a greater than 99.9% probability that the model was a good fit to the data.

2.3. *EUVE* data

RE J1034+396 was observed with the Deep Survey Spectrometer (DS/S) on board *EUVE* from 14 April 1997 UT 05:35:04 to 20 April 1997 UT 01:03:07 for a total of approximately 100 ks. The observation was part of a simultaneous *EUVE*/*Beppo-SAX* campaign.

The DS/S (Welsh et al. 1990) is equipped with a broad band imaging detector (covering the 66−178 Å or 0.07 − 0.18 keV band in the Lexan/B filter) and three spectrometers (Hettrick & Bowyer 1983; Abbot et al. 1997) covering the "short" (SW: 70 − 190 Å, 0.06 − 0.18 keV), "medium" (MW: 140 − 380 Å) and "long" (LW: 280 − 760Å) EUV wavelengths. This configuration allows simultaneous imaging and spectroscopy with a spatial resolution of $\sim$ 1 arc min and a spectral resolution of $\lambda/\Delta\lambda \sim 200$ at the short wavelengths.

RE J1034+396 was observed 0.2° off-axis in order to avoid the DS dead-spot and to extend the spectrum toward shorter wavelengths ($\lambda_{\rm min} \sim 66$ Å) with respect to a regular on-axis observations ($\lambda_{\rm min} \sim 72$ Å). [The DS dead-spot is a small region of reduced gain and detector quantum efficiency near the center of the DS detector, caused by the observation of the very bright EUV source HZ 43 (Sirk 1993).]

2.3.1. Light-curve

We extracted the light-curves from the DS time-ordered event list using the *EUVE* Guest Observer Center software (IRAF/EUV package) and other

IRAF timing tasks adapted for *EUVE* data. After correcting the data for instrumental dead-time, telemetry saturation, vignetting and eliminating intervals of high particle background, the total effective exposure is 97061 s.

We counted the source photons in a circle of 1.1′ radius, and we estimated the background in a concentric annulus with inner and outer radii of 1.5′ and 3.8′ respectively. The extraction region includes more than 98% of the DS point spread function (Sirk et al. 1997). The effective area of the DS instrument (25 cm^2 at $\lambda = 85$ Å), is more than 10 times larger than the spectrometer effective area at this wavelength and a good detection of the source (average signal-to-noise ratio (SNR) ~ 4.9) was obtained during each orbit. Figure 2 shows the light curve binned over one average *EUVE* orbit (about 5544 s). Since the *EUVE* instruments are shut down during satellite daytime (around 2/3 of the total orbital time for EUVE 550 km circular orbit with an inclination of 28°) and passages through regions of high particle background (such as the South Atlantic Anomaly) the average effective exposure per orbit is approximately 1000 s, after discarding the bins with effective exposure less than 200 s.

The average count rate over the entire observations is 0.038 ± 0.001 counts s^{-1}. As a comparison RE J1034+396 was observed twice before by *EUVE*: during the all-sky survey in 1992-1993 it had a count rate of 0.023 ± 0.007 in $\sim$ 1600 s of observation (Fruscione 1996) and again serendipitously on 27 December 1993 for an effective exposure time of $\sim$ 5000 s; the count rate then was 0.029 ± 0.003 (Fruscione, private communication). During the observation described in this paper (April 1997), RE J1034+396 was in a relatively bright state, ∼60% brighter than in the all-sky survey and ∼30% brighter than in December 1993.

As immediately visible from the light-curve, the EUV flux from RE J1034+396 remained effectively constant for the 5 days of observation and in fact a χ^2 test for a constant source on the entire data set (excluding intervals with effective exposure below 200 s) gives a value of 51 for 75 degrees of freedom, corresponding to a $\sim$ 1% probability that the source varied during the six days of this observation.

2.4. *ROSAT* HRI images

Since the re-discovery of the active nucleus in RE J1034+396 by the *ROSAT* Wide Field Camera in 1990, several observations have been made in the soft and medium X-rays and a log of the available data to date is given in Table 1.

A measurement of the soft X-ray flux from RE J1034+396 was made with the HRI on *ROSAT* in 1996 November and yielded a count rate of 0.61 ± 0.02 count s^{-1} with no evidence for variability for the duration of the observation (∼30 ks). The full width at half maximum (FWHM) of the profile of RE J1034+396 was 7 arc sec. The point spread function (PSF) of an unresolved on-axis source observed by the HRI has a FWHM between ∼5.1 and 7.4 arc sec, thus the soft X-ray emission of RE J1034+396 in the *ROSAT* HRI was consistent with a point source.

A previous HRI observation of RE J1034+396 was made in 1994 November 20. We measure a count rate of 0.49 ± 0.02 from these data, thus the soft X-ray flux had increased by ∼20% in the two years since the 1994 pointing. This is consistent with *EUVE* observations which showed an increase between 1992/1993 and 1997 (see Section 2.3.1).

2.5. *ASCA* observations

RE J1034+396 has been observed on two occasions by *ASCA*, in 1994 November (coincident with the first *ROSAT* HRI observation) and six months later in 1995 May. The first dataset was analyzed by Pounds, Done & Osborne (1995) but the second is unpublished to date. We present the 1995 data here and re-analyze the 1994 spectra to ensure a consistent approach towards the data reduction when comparing observations.

Both sets of SIS observations were taken in 1-CCD mode. The GIS source spectra were extracted using a circle of radius 4 arc min. The GIS background regions were selected from a position opposite that of RE J1034+396, i.e. at the same radial distance, and with a circle of radius 6.7 arc min. The SIS spectra were extracted using a circle of radius 3 arc min and a nearby circular region of the SIS chips was used for the background. The background light-curves were used to check for and discard any periods of anomalous data before the spectra were extracted.

The background subtracted light-curves of the

target were examined for signs of significant variability. None was seen in the 72020000 data [consistent with the results of Pounds, Done & Osborne (1995)]. In the 72020010 observation, there is a suggestion of variability at the 20-30% level, although a χ^2 test indicates that this cannot be distinguished from flux at a constant level. The count rate of RE J1034+396 in 1995 May was consistent with that six months earlier in 1994 November at the 2σ level.

The reduced spectra were fitted with a combination of power-law and thermal models, using the XSPEC spectral fitting package (Version 11.00) and the results are given in Table 1. The fitting ranges were 1.0 to 10 keV for the GIS and 0.7 to 10 keV for the two SIS. In all the fits, a Galactic column density of 1.5×10^{20} cm^{-2}, interpolated from the maps of Stark et al. (1992), was assumed. For the earlier 72020000 observation, the lowest χ^2_νs were obtained for the two power-law and two blackbody plus power-law fits (full details are given in the table). For all fits, the best fit intrinsic column density converged to 0, indicating little if any absorption local to the AGN. The slopes of the hard X-ray power-law for the two best-fitting models were α ~0.7-0.8 which is typical of AGN in general (Mushotzky 1984; Comastri et al. 1992) and *not* significantly softer as suggested by Pounds, Done & Osborne (1995).

The second dataset, 72020010, was observed for only one-third as long as the earlier one, thus the fits are more poorly constrained. Only a single power-law model gave an acceptable fit to the data if the intrinsic column was allowed to be free: for the other three models tried, the intrinsic column converged to a few times 10^{21} cm^{-2}. Such high column densities were in turn offset by un-physically strong un-absorbed components, suggesting some flattening of the spectrum towards lower energies. A broken power-law model with no intrinsic column did give an improved fit over a single power-law. The single power-law fit could not be improved by the addition of a bremsstrahlung or blackbody component however.

The 72020010 data were well-fitted with the best-fitting two blackbody plus power-law model for the earlier data, giving a χ^2_ν=0.95 for 156 degrees of freedom (ie having fixed all parameters except the normalizations). This suggests that there was no significant spectral variability either between the two *ASCA* observations.

2.6. *Beppo-SAX* observations

RE J1034+396 was observed on 1997 April 18 and 19 with the *Beppo-SAX* Narrow Field Instruments, the Low Energy Concentrator Spectrometer [LECS; 0.1-10 keV (Parmar 1997)], the Medium Energy Concentrator Spectrometer [MECS; 1.3-10 keV (Boella et al. 1997)], the High Pressure Gas Scintillation Proportional Counter [HPGSPC; 4-60 keV (Manzo et al. 1997)] and the Phoswich Detector System [PDS; 13-200 keV (Frontera et al. 1997)]. The source was not detected in the high energy instruments thus we report here the analysis of the LECS and MECS only.

The observations were performed with all three MECS units and data from these were combined together after gain equalization. The LECS is operated during dark time only, therefore LECS exposure times are usually smaller than MECS ones by a factor 1.5-3 (a factor of 2 for RE J1034+396). Standard data reduction was performed using the SAXDAS software package (www.sdc.asi.it/software/saxdas). In particular, data are linearized and cleaned from Earth occultation periods and unwanted periods of high particle background (satellite passages through the South Atlantic Anomaly). The LECS, MECS and PDS backgrounds are relatively small and stable (variations of at most 30% during the orbit) due to the satellite's low inclination orbit (3.95°). Therefore data quality depends little on screening criteria such as Earth elevation angle, Bright Earth angle and magnetic cut-off rigidity (we accumulated data for Earth elevation angles $> 5°$ and magnetic cut-off rigidity $> 6°$).

We extracted the LECS spectrum from 8 arc min radius regions. This radius maximizes the signal-to-noise ratio below 1 keV in the LECS. The MECS image is *not* consistent with the instrument PSF and the spatial analysis will be presented elsewhere (Fiore et al., in preparation). We have used source extraction radii of 2 and 3 arc min to avoid as much as possible problems of confusion or the contribution of extended emission. The results for 2 and 3 arc min extraction radii were consistent with each other and we report in the following, those obtained with the 3 arc min extraction radius.

The LECS and MECS internal backgrounds depend on the position [see Chiappetti et al. (1998), and the BeppoSAX Cookbook, www.sdc.asi.it/software/cookbook]. Background spectra have then been extracted from high Galactic latitude 'blank' fields from regions equal to the source extraction region, in detector coordinates. We have checked whether the mean level of the background in these observations is comparable with the mean level of the background in the quasar observations using source free regions at various positions in the detectors. In the LECS the mean local background is consistent with the 'blank' field mean background. In the MECS we found that the local background is higher than the blank field background by 7%. We have verified that the excess is constant in energy. We then scaled by the same amount the blank field background spectra before subtraction.

Table 3 gives the observation dates, LECS and MECS exposure times and the detected count rate in each instrument.

Spectral fits were performed using the XSPEC 9.0 software package and public response matrices as from the 1997 August 31^{st} issue. Spectra were always re-binned following two criteria: a) to sample the energy resolution of the detectors with four channels at all energies where possible, and b) to obtain at least 20 counts per energy channel. This allows the use of the χ^2 statistic in determining the best fit parameters, since the distribution in each channel can be considered Gaussian while avoiding possible systematic errors due to the linearity in the spacing of the original sampling. Constant factors have been introduced in the fitting models in order to take into account the inter-calibration systematics between instruments (Fiore et al. 1998). The expected factor between LECS and MECS is about 0.9. In the fits we then assume the MECS as reference instruments and constrained the LECS parameter to vary in the small range 0.7-1.1. The energy range used for the fits are: 0.1-4 keV for the LECS (channels 11-400), 1.65-10 keV for the MECS (channels 37-220)

2.6.1. Spectral analysis

LECS and MECS spectra were fitted with a number of models: single power-law, broken power-law, 2 power-laws and power-law plus disc black body. In all cases the emission spectrum was reduced at low energy by a cut-off due to neutral gas along the line of sight. The column density of the gas was always constrained to be greater than or equal to the Galactic value along the line of sight of 1.5×10^{20} cm^{-2}.

Table 4 gives the best fit parameters along with the χ^2 obtained in each case. To ease the comparison of the *Beppo-SAX* observation with previous ROSAT and ASCA observations we have also fitted the single LECS and MECS spectra with a power-law model limited to the ranges 0.1-2 keV and 2-10 keV.

The 90% limit on a 6.4 keV(6.7 keV) iron Kα line in the *BeppoSAX* data is 165 eV (210 eV).

2.6.2. Spectral curvature

Figure 3 shows the fit with a single power-law: positive residuals are evident above 3-4 keV . The spectrum is clearly flattening above this energy. The significance of the flattening is demonstrated in Figure 4 which shows the contour plot for the soft and hard slopes of the broken power-law model. The figure shows that the soft index, Γ_{low} is softer than the hard, Γ_{high} at greater than 99% significance.

The fits with two power-laws, a broken power-law and a blackbody plus a power-law all give a χ^2 which is significantly smaller than a single power-law (Table 4). The blackbody plus power-law model produces an acceptable χ^2 and a best fit absorbing column density lower than Galactic, unlike the other two models. Therefore either we are measuring a small column in the host galaxy of RE J1034+396, or the emission spectrum has a curvature also at low energy. While the former case is certainly possible, the possibility of a low energy turn down of the emission spectrum is intriguing, because it may suggest a small black hole mass, if the low energy emission is interpreted in terms of optically thick disk emission.

Indeed the soft X−ray spectrum is best fitted with two blackbodies which mimic a multi-temperature disc model. This result is consistent with the analysis of the *ROSAT* PSPC data by Puchnarewicz et al. (1995), who found a significant hardening of the 0.1-2 keV spectrum at low energies, when the column density was fixed at the Galactic value.

The spectrum was also fitted with a bremsstrahlung

plus power-law model which gave a χ^2 of 75.5 (for 94 degrees of freedom). Thus although a bremsstrahlung form for the soft X-ray component cannot be ruled out, the two-blackbody representation does produce the lowest χ^2_ν. Furthermore, a bremsstrahlung form for the soft X-ray component is not generally popular, because the implied extent of the optically-thin gas would be much larger than suggested by the variability of most NLS1s.

The preferred slope of the hard X-ray power-law continuum depends on the form assumed for the ultra-soft component. For the best-fitting two blackbody plus power-law model, the hard power-law is best represented by a slope α=1.2. This is slightly harder than that measured by Pounds, Done & Osborne (1995) but only slightly softer than that of AGN in general (where $\alpha \sim 1$). Our analysis of the *ASCA* data suggest a slope for the hard X-ray power-law, α, between 0.7 and 1.3, depending on the model assumed for the soft component.

Comparing the *Beppo-SAX* spectrum with the *ASCA* data, we find that the flux and spectral form of all three observations are consistent within 90%.

3. Model fits to the optical to X-ray continuum

In spite of its historical significance as one of the first NLS1s with a strong ultra-soft component to be reported, RE J1034+396, unlike many others in its class, has exhibited a remarkable degree of flux and spectral stability. In this paper, we present a comprehensive review of measurements of RE J1034+396 in the EUV to X-rays over 6 years, and over this period it has shown changes on long time-scales of up to 60% (compared to eg. RE J1227+164 whose flux changed by a factor of 70). On short time-scales, no significant changes have been observed. Thus, in a study such as this where we wish to fit non-simultaneous optical to X-ray data of a NLS1, RE J1034+396 is the prime candidate. Obviously simultaneous optical to X-ray data, such as that which will be provided by the Optical Monitor and EPIC on XMM Newton, would be the ideal, but until such data are obtained, the quasi-simultaneous observations presented here provide the best available.

The 'nuclear' spectrum of RE J1034+396 is illustrated in Figure 5. This is made up of the point-source component extracted from the optical data (Section 2.1), the *HST* spectrum (Section 2.2) and the *Beppo-SAX* spectrum (Section 2.6).

We have assumed that the optical-UV-X-ray emission originates primarily in a geometrically thin accretion disk around a rotating supermassive black hole. The radial temperature of the standard, Keplerian disk is calculated given the black hole mass and the accretion rate. We approximate the disk emission by local blackbody emission, which is modified by electron scattering in the disk atmosphere (Czerny & Elvis 1987). Relativistic corrections have been applied to the disk emission following Laor et al. (1989).

We fit the optical to X-ray spectrum of RE J1034+396 using a grid of accretion disk models parameterized by a central black hole mass (M_{bh}), accretion rate ($\dot{M}$) and inclination angle (Siemiginowska et al. 1995). Because there is no signature of the BBB in the UV spectrum of RE 1034+396 we also add a power-law component to the disk emission in order to describe the optical/UV continuum. We normalized a power law at 2 keV to 8×10^{42} erg s^{-1} with a slope fixed to $\alpha = 1.15$ to connect the near IR and hard X-ray points (see Figure 5). The implications of a possible physical significance of this component are discussed in Section 4.2.

The fact that the spectral turn-over is detected in the soft X-ray band (Section 2.6.2) can be used to constrain the minimum black hole mass required for the source. Assuming that the peak seen in the soft X-ray spectrum is related to the maximum effective temperature of the optically thick disk, then the physical radius at which this emission is generated is given by (Frank, King & Raine 1992):

$$\sigma T_{\rm eff}^4 = \frac{3GM\dot{M}}{8\pi R_{max}^3}(1-\sqrt{\frac{3R_{Sch}}{R_{max}}}) \qquad (1)$$

$$R_{max} = \frac{49}{36}R_{Sch} \qquad (2)$$

where $T_{\rm eff}$ is the effective temperature, $R_{Sch} = 2GM_{bh}/c^2$ is the Schwarzschild radius of the black hole and R_{max} is the radius where the maximum temperature is reached.

At a given effective temperature the disk contributes the most of the emission to the frequency

given by Siemiginoswka & Czerny (1989) and Czerny & Elvis (1987):

$$kT_{\rm eff} = 1.625h\nu \quad (3)$$

This allow us to link the turn-over observed in the spectrum with the central black hole mass. Our approximation assumes that the disk is optically thick and the entire spectrum is described by local blackbody emission. However, at high temperatures the disk photons are re-scattered by electrons in the atmosphere of the disk. Some photons gain energy and contribute to the soft X-ray spectrum. This modification allows to see the turn-over at higher frequencies, so a higher black hole mass is allowed.

For a turn-over at $\sim$ 0.25keV and an accretion rate corresponding to the Eddington luminosity, the mass derived from the above equations is $\sim 10^4 M_\odot$. This mass can be larger if most of the observed photons are Comptonized in the disk atmosphere. The UV photons can gain energy up to a mean value of $3kT$. This is to $\sim$ 0.25 keV for photons at the spectral peak of RE J1034+396. If we take this temperature into account then the central black hole mass is estimated to be of the order $6 \times 10^6 M_\odot$, again assuming the critical accretion rate.

Using the optical to X-ray data presented here, best-fitting parameters for the black hole mass and accretion rate have been derived by constructing χ^2_ν grids for models compared with the data over a range of inclination angles. In Figure 6 we show the confidence intervals for accretion rate and black hole mass at inclinations [cos(inc)] of 0.25, 0.5, 0.75 and 1.0 [where cos(inc)=1.0 corresponds to a face-on disk]. The face-on configuration is ruled-out: note also that, in general, the highest accretion rates are not consistent assumptions built into the model. The results suggest that RE J1034+396 contains a relatively small black hole mass, with the best fitting value of $\sim 5 \times 10^6 M_\odot$. The accretion rates are relatively high, but consistent with the model assumption. The best accretion rate value is found to be equal to 0.4 $\dot{M}_{\rm Edd}$ for a relatively edge-on inclination angle of cos(inc)=0.25. In Figures 7 and 8, we show some of the fits to the nuclear spectrum at cos(inc)=0.25 and 0.5, around the best-fitting values.

One problem with modeling these data, is that the signal to noise ratios in the optical and UV, and the number of available data points, are much higher than that in X-rays. This results in an imbalance in the significance of the optical/UV data over the X-rays in the χ^2_ν statistic, despite the physical significance of the form of the X-ray spectrum.

To establish which parameters the high energy data alone would prefer, we have repeated this fitting procedure using only the X-ray data. The resulting χ^2_ν grids are consistent with those for the full optical/UV/X-ray data, with a minimum at $M_{bh} = 5 \times 10^6 M_\odot$, $\dot{M}$=0.4 $\dot{M}_{\rm Edd}$ and cos(inc)=0.25, and the face-on geometry ruled out.

As a further check on the robustness of the results, we have also 'matched' the resolution of the optical/UV data to the X-rays. This was done by binning the spectra so that the number of optical/UV data points per frequency decade was similar to that in the X-ray spectrum. Although this reduces the error on the measurement of the flux in each bin, the overall error remains dominated by uncertainties in the absolute flux determination and by the effects of any spectral variability. Thus, the errors on the binned optical/UV data were also assumed to be $\pm$20%. Again, the grids for the binned optical/UV data were consistent with those for the full optical/UV/X-ray data as above. The χ^2_ν's were generally higher at each point in the grids, but the minima had values of $\sim$1.

4. Discussion

The *HST*-FOS data and quasi-simultaneous 0.1-10 keV spectrum measured by *Beppo-SAX* provide very tight constraints on the form of what we assume to be the BBB (i.e. a single component which would normally encompass the optical/UV BBB and the soft X-ray excess) in RE J1034+396. No sign of significant emission from the BBB is seen in the FOS spectrum down to $\sim$1250 Å, while the LECS spectrum measures a very steep and relatively strong soft X-ray component. There is also evidence for a flattening towards the lowest energies in the X-ray spectrum (below $\sim$0.3 keV), confirming earlier *ROSAT* PSPC observations. Thus the unusually high temperature of the BBB in RE J1034+396 makes the source unique for two reasons: *(1)* the BBB is shifted out of the opti-

cal/UV range completely; and *(2)* assuming *no* cold gas absorption intrinsic to RE J1034+396, the high energy turnover of the BBB is observed in soft X-rays at $\sim$0.25 keV.

RE J1034+396 is important in one further respect: it shows no evidence for significant variability on short time-scales ($\sim$days), and only moderate variability on long time-scales (months to years). This is contrary to the nature of Seyferts in general, where sources with very soft X-ray spectra tend to show large amplitude variability on short time-scales, while harder sources vary less [see eg. Fiore et al. (1998) and references therein].

4.1. Black hole mass and accretion rate

This unique set of observational properties, and the availability of quasi-simultaneous data, has enabled us to place meaningful constraints on the essential parameters of RE J1034+396, ie. the black hole mass, accretion rate and inclination of the AD to our line of sight. The χ^2_ν grids favor almost Eddington accretion rates ($\sim 0.4 \mathrm{M_{Edd}}$) onto a relatively low mass black hole ($\mathrm{M}_{bh} \sim 5 \times 10^6 \mathrm{M}_\odot$), for a disk inclined relatively edge-on (ie. 75° from the axis of the disk). This is consistent with the hypothesis of Pounds, Done & Osborne (1995), who suggested that RE J1034+396, and NLS1s in general, were systems analogous to Galactic Black Hole Candidates (GBHCs). Models of GBHCs predict that, in their 'high-state', the accretion rate onto the black hole is high, resulting in a strong soft thermal component and a relatively soft, fluctuating hard power-law.

If, in the case of NLS1s, the matter was accreting at high rates onto a relatively low mass black hole, this would also result in a relatively high temperature for the inner edge of the AD. Thus a very hot, soft X-ray component would be observed in NLS1s when compared to other AGN. In addition, the low-mass black hole might result in a low-velocity broad line region (BLR), either because the clouds were moving more slowly due to the weaker gravitational potential, or because the emitting regions were located further out (which in turn might be due to the weaker gravitational field and/or the unusual form of the incident ionizing continuum).

Our results are consistent with this idea of high accretion onto a relatively low mass black hole. There is one possible problem that should be addressed however, and that is the inclination of the AD. The fits prefer an almost edge-on disk ($\sim 60 - 70°$), which is not unexpected as such, since the probability of observing an AD in soft X-rays, assuming isotropic emission of the soft X-ray flux, is proportional to the sine of the inclination angle. This in itself is not a problem, but one might naively expect any molecular torus to lie roughly co-planar with the AD. Given that the opening angle of such tori is thought to be about 45° and the optical depths implied are high [$\sim 10^{24}$ cm^{-2}; see eg. Antonucci (1993)], this would effectively block out any soft X-ray or UV emission from the disk, yet significant amounts of both are observed. Therefore if our modeling is correct, either the molecular torus is geometrically-thin, optically-thin, patchy or absent altogether, or the planes of the AD and the torus are more orthogonal than coincident.

Boller et al. (1997) suggested that NLS1s in general may contain disks viewed relatively *face-on* which would contradict the results of our modeling. However, they based this hypothesis on the high levels of variability seen in many NLS1s (and in IRAS 13224–3809 in particular) and RE J1034+396 has shown only relatively small changes over long time-scales. Thus while the variability may be related to the inclination of the disk, our model fits suggest that the ultra-soft X-ray emission, the low-velocity BLR and the direct or indirect link between the two, may not be.

4.2. The optical/UV 'power-law' continuum

When the FOS data are combined with the spectrum of the nuclear optical continuum (see Section 3; Fig. 5), we find a very flat, power-law-like component with a spectral index, $\alpha \sim 1$, covering the 8000 Å to 1200 Å range. There is no sign of any rise towards the blue in this region (which is characteristic of the BBB), and the emission from the host galaxy of the AGN has been removed. The residual component appears to be non-thermal in nature. It cannot be due to the sum of thermal dust components because dust grains sublime at 10^5 K and their emission is negligible at wavelengths short-ward of 1μm. Therefore, this represents the first unambiguous

detection of a non-thermal optical/UV continuum component in any AGN.

When modeling the optical to X-ray data, it was necessary to assume an underlying optical to X-ray power-law, in addition to the accretion disc component, to fit the optical/UV continuum *and* the hardening of the X-ray spectrum towards harder energies. The slope of this power-law was α=1.15, slightly softer than that in the optical/UV alone. The resulting deficit in the UV between the data and the power-law was well-modeled by the accretion disc component (see Figs 7 and 8). Thus the data and the modeling presented here, are consistent with the presence of a single power-law component which underlies the optical to X-ray spectrum of RE J1034+396.

The existence of a single power-law component connecting the IR to the X-rays has been suggested before (Malkan 1984; Elvis et al. 1986; Carleton et al. 1987), although the 'bare' power-law, such as we have observed in RE J1034+396, has not (to our knowledge) been observed, due to the dominance of the 'thermal' components in the optical and IR, respectively. The IR to UV continuum is generally thought to be the sum of thermal components from dust and the accretion disk. The hard X-ray power-law is considered to be physically unrelated and produced by inverse Compton scattering of blackbody photons from the disk in a surrounding hot corona. Previous claims of a continuous IR-to-X-ray power-law component have been based on correlations between IR and X-ray luminosities (Malkan 1984; Carleton et al. 1987) and extrapolations of the medium X-ray spectrum into the IR (Elvis et al. 1986). In addition, Fernandes, Sodré & Vieira da Silva (2000) found evidence for a stable, underlying red continuum component in the optical spectra of PG Quasars. The direct observation of the optical/UV power-law component in RE J1034+396 makes this a prime target for the study of broadband, non-thermal emission in Seyfert galaxies.

Using *ROSAT*-PSPC, optical, *IUE* and archival *IRAS* data, Puchnarewicz et al. (1995) also discussed the possibility of an underlying IR to X-ray power-law component in RE J1034+396. These data suggested a softer slope to the power-law however (α $\sim$1.4), due to the lack of any constraint in hard X-rays (E >2keV) and probable contamination of the optical spectrum by the host galaxy.

The similarity of this component to that observed in BL Lac objects led Puchnarewicz et al. (1995) to hypothesize that there may be some kind of 'mini-BL Lac' activity in RE J1034+396. Although subsequent optical spectropolarimetry of RE J1034+396 revealed an upper limit on the polarization of the continuum of 0.4% (Breeveld & Puchnarewicz 1998), the 'duty cycle' of X-ray selected BL Lac objects (i.e. the fraction of time spent in periods of significant variability and polarization) is $\sim$40% or less (Januzzi, Smith & Elston 1994; Heidt & Wagner 1998). Thus it is possible that RE J1034+396 does have a BL Lac component which dominates in the optical/UV, but is currently in a quiescent state.

5. Conclusions

We have presented a comprehensive study of the narrow-line Seyfert 1 galaxy RE J1034+396, spanning the optical to X-rays and six years of observations. Focusing on quasi-simultaneous *Beppo-SAX*, *HST*, *EUVE* and optical data taken in early 1997, we have *(1)* measured the soft and hard X-ray components simultaneously for the first time using *Beppo-SAX*; *(2)* placed tight constraints on the form of the big blue bump using *HST*, *EUVE* and *Beppo-SAX*; *(3)* separated out the nuclear component from the host galaxy in the optical; and *(4)* fitted the optical to X-ray nuclear continuum with the combination of an accretion disk and an underlying power-law, to constrain the black hole mass, accretion rate and inclination of the accretion disk in RE J1034+396.

Coverage of the widest possible range in X-rays, particularly at soft energies, is of prime importance for NLS1s, because of their strong ultra-soft components. These *Beppo-SAX* data, which cover the 0.1 to 10 keV range, provide significant constraints on the shape, and thus the physical nature, of the X-ray spectrum in RE J1034+396. Our analysis of the *Beppo-SAX* spectrum reveals a significant hardening of the X-ray spectrum above $\sim$3 keV and that two blackbodies, with $kT_{\rm eff}$=60 eV and 160 eV best represent the ultra-soft X-ray component, consistent with multi-temperature emission from an optically-thick accretion disc. We do not find any compelling evidence to suggest that the hard X-ray power-law in

RE J1034+396 is significantly softer than that of non-NLS1 AGN. There is the suggestion of a low-energy flattening in the *Beppo-SAX* data, which was also observed in the earlier *ROSAT* PSPC spectrum. This in turn implies a high temperature for the inner edge of the accretion disk, and thus a low black hole mass (which is also borne out by the modeling).

The results of fitting the optical to X-ray nuclear continuum have shown that the data prefer relatively high mass accretion rates ($\sim$0.3 to 0.7 $\dot{M}_{\rm Edd}$) onto a low mass black hole (M_{bh} $\sim$2-10×10^6 $M_\odot$) at high inclination angles (ie. preferably edge-on, $\sim 60-70^\circ$ away from the axis of the disc). The very low intrinsic columns implied by the X-ray fits suggest that any molecular torus must either be optically thin, geometrically thin, or lie out of the plane of the accretion disk so that it does not obscure our line of sight.

The optical to X-ray nuclear continuum *requires* the presence of a flat, power-law-like component in the optical/UV. This is consistent with an extrapolation to the hard X-ray spectrum, although an independent origin for the hard X-ray power-law cannot be ruled out. The existence of such a component has been proposed before, but we believe that this is the first direct observation, by virtue of the unusually hot big blue bump in RE J1034+396. It appears to be stable and unpolarized and we speculate that it may be a BL Lac-type component which is currently in the quiescent stage of its duty-cycle.

We thank the anonymous referee for comments which improved the paper. This research has made use of data obtained through the High Energy Astrophysics Science Archive Research Center Online Service, provided by the NASA/Goddard Space Flight Center. This work is partly supported by the Italian Space Agency, contract ARS/98–119 and by the Ministry for University and Research (MURST) under grant COFIN–98–02–32. This research has made use of data obtained from the Leicester Database and Archive Service at the Department of Physics and Astronomy, Leicester University, UK. The WHT is operated on the island of La Palma by the Isaac Newton Group in the Spanish Observatorio del Roque de los Muchachos of the Instituto de Astrofisica de Canarias.

REFERENCES

Abbott, M., Boyd, W., Jelinsky, P., Christian, C., Miller-Bagwell, A., Lampton, M., Malina, R. F. and Vallerga, J. V. 1997, ApJS, 107, 451

Antonucci R., 1993, Ann. Rev. Astron. Astroph., 31, 473

Boella G. et al., 1997, A&AS, 122, 327

Boller Th., Brandt W. N., Fabian A. C. and Fink H., 1997, MNRAS, 289, 393, astro-ph/9703114

Boller Th., Brandt W. N. and Fink H., 1996, A&A, 305, 53, astro-ph/9504093

Brandt W. N., Fabian A. C. and Pounds K. A., 1996, MNRAS, 278, 326

Breeveld A. A. and Puchnarewicz E. M., 1998, MNRAS, 295, 568

Carleton N. P., Elvis M., Fabbiano G., Willner S. P., Lawrence A. and Ward M., 1987, ApJ, 318, 595

Chiappetti L. et al., 1998, qqin "The Active X-ray Sky", L Scarsi, H. Brandt, P Giommi and F. Fiore (Eds.), Nuclear Physics B Proc. Suppl. 69/1-3, 610

Comastri A., Setti G., Zamorani G., Elvis M., Wilkes B. J., McDowell J. C. and Giommi P., 1992, ApJ, 384, 62

Czerny B. and Elvis M., 1987, ApJ, 321, 305

Elvis M., Green R. F., Bechtold J., Schmidt M., Neugebauer G., Soifer B. T., Matthews K. and Fabbiano G., 1986, ApJ, 310, 291

Fernandes R. C., Sodré L. & Vieira da Silva L., 2000, ApJ, in press]

Fiore F., Laor A., Elvis M., Nicastro F. and Giallongo E., 1998, ApJ, 503, 607

Frank J., King A. and Raine D., 1992, in *Accretion Power in Astrophysics, Second Edition*, Eds. R. F. Carswell, D. N. C. Lin and J. E. Pringle, Pub. Cambridge University Press.

Frontera F., Costa E., dal Fiume D., Feroci M., Nicastro L., Orlandini M., Palazzi E. and Zavattini G., 1997, A&AS, 122, 357

Fruscione, A. 1996, ApJ, 459, 509

Heidt J. and Wagner S. J., 1998, A&A, 329, 853

Hettrick, M.C. and Bowyer, S. 1983, Appl. Opt., 3921

Januzzi B. T., Smith P. S. and Elston R., 1994, ApJ, 428, 130

Laor A. and Netzer H., 1989, MNRAS, 238, 897

Malkan M. A., 1984, in *X-ray and UV Emission from Active Galactic Nuclei*, ed. W. Brinckmann and S. Trumper (MPIfR), 121

Manzo G., Giarrusso S., Santangelo A., Ciralli F.,,Fazio G., Piraino S. and Segreto A., 1997, A&AS, 122, 341

Mushotzky R. F., 1984, Advances in Space Research, 3, 10-13, 157

Parmar A. N., Martin D. D. E., Bavdaz M., Favata F., Kuulkers E., Vacanti, G., Lammers U., Peacock A. and Taylor, B. G., 1997, A&AS, 122, 309

Pounds K. A., Done C. and Osborne J. P., 1995, MNRAS, 277, L5

Puchnarewicz E. M., Mason K. O., Córdova F. A., Kartje J., Branduardi-Raymont G., Mittaz J. P. D., Murdin P. G. and Allington-Smith J., 1992, MNRAS, 256, 589

Puchnarewicz E. M. Mason K. O., Siemiginowska A. and Pounds K. A., 1995, MNRAS, 276, 20

Puchnarewicz, E. M. Mason, K. O. and Siemiginowska, A. 1998, MNRAS, 293, L52

Siemiginowska A., Czerny B., 1989, MNRAS, 239, 289

Siemiginowska A., Kuhn O., Elvis M., Fiore F., McDowell J. and Wilkes, B. J., 1995, ApJ, 454, 77

Sirk, M. M., 1993, in "American Astronomical Society Meeting", 182, 4132

Sirk, M. M., Vallerga, J. V., Finley, D. S., Jelinsky, P. and Malina, R. F., 1997, ApJ, 110, 347

Stark A. A., Gammie C. F., Wilson R. F., Ball J., Linke R. A., Heiles C. and Hurwitz M., 1992, ApJS, 79, 77

Welsh, B. Y., Vallerga, J. V., Jelinsky, P., Vedder, P. W., Bowyer, S. and Malina, R. F. 1990, Opt. Eng., 29, 752

This 2-column preprint was prepared with the AAS LaTeX macros v5.0.

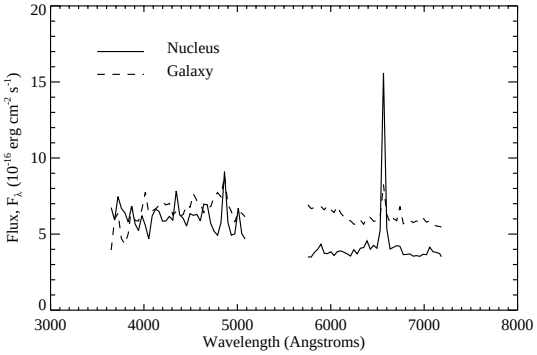

Fig. 1.— The separate nuclear (plotted as a solid line) and galactic (dashed line) components of the optical (*WHT*) spectrum of RE J1034+396.

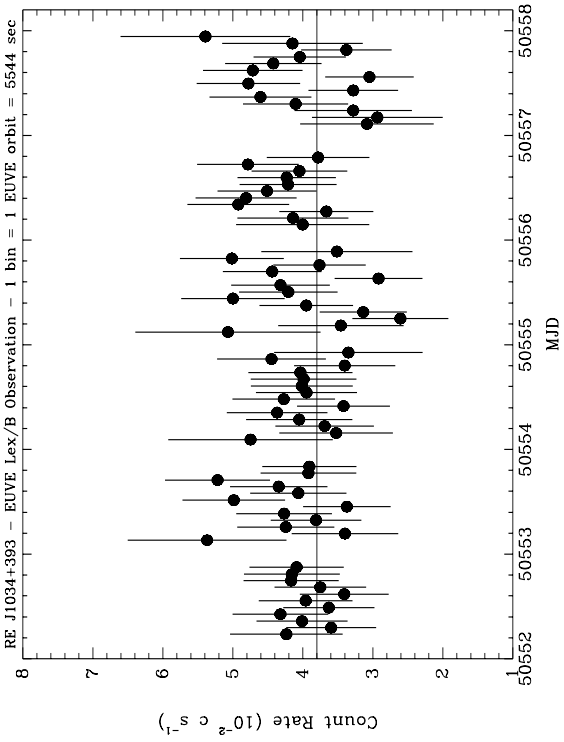

Fig. 2.— The *EUVE* light-curve of RE J1034+396.

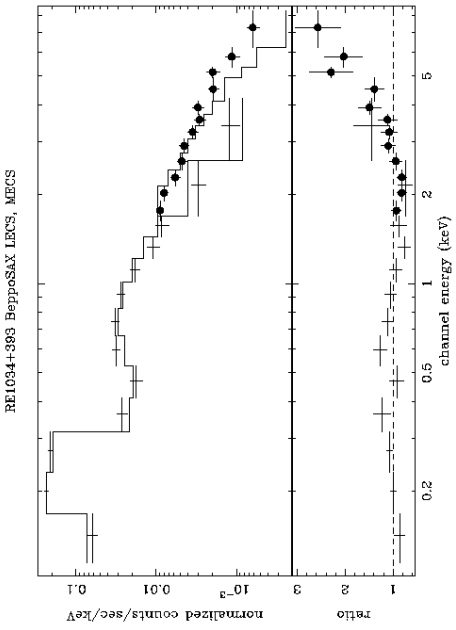

Fig. 3.— The 0.1-10 keV BeppoSAX LECS, MECS spectra of RE J1034+396 fitted with a power-law model reduced at low energy by Galactic absorption. Lower panel shows the ratio between data and model. Error bars are 1σ (68%).

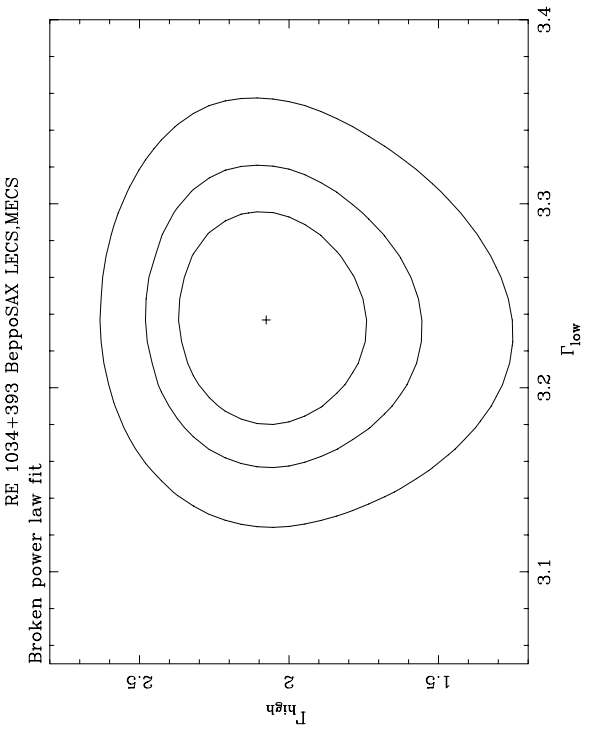

Fig. 4.— The $\Gamma_{low} - \Gamma_{high}$ contour plot for a broken power-law fit to the LECS and MECS 0.1-10 keV data of RE J1034+396. Contours are drawn at 68%, 90% and 99% significance for two interesting parameters.

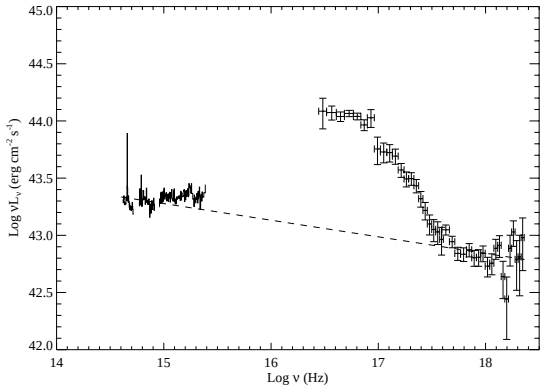

Fig. 5.— The optical to X-ray spectrum of RE J1034+396, combining the WHT, *HST*-FOS and *Beppo-SAX* data. The underlying optical to X-ray power-law continuum used in the fits is also shown as a dashed line. Errors are 1σ (68%).

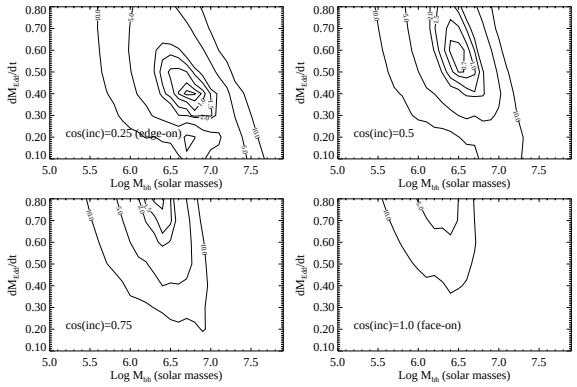

Fig. 6.— χ^2_ν contour plots for the AD plus power-law models when compared with the optical, UV and X-ray data for RE J1034+396.

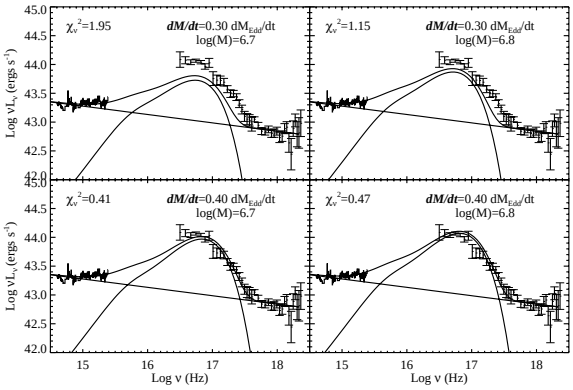

Fig. 7.— AD plus power-law fits to the optical to X-ray data at an angle of inclination, cos(inc)=0.25.

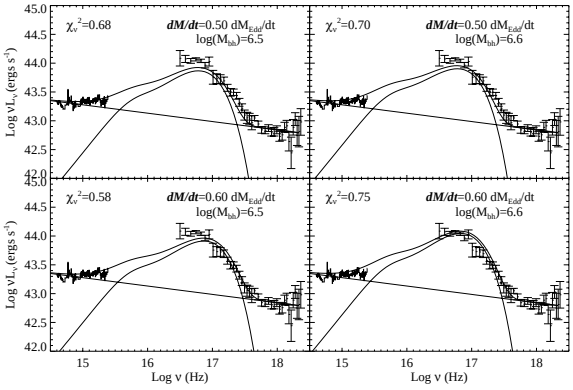

Fig. 8.— AD plus power-law fits to the optical to X-ray data at an angle of inclination, cos(inc)=0.5.

TABLE 1

LOG OF EUV AND X-RAY OBSERVATIONS

Date	Instrument	Observation No.	Exposure time (ks)	Count rate 10^{-2} count s^{-1}	Reference
1991 Nov 18	*ROSAT* PSPC	RP700551	330	3	(1)
1992-1993	*EUVE* All-Sky Survey		1.6	2.3±0.7	(2)
1993 Dec 27	*EUVE* DS/S		5	2.9±0.3	(3)
1994 Nov 20	*ROSAT* HRI	RH701982	1.6	49±2	(4)
1994 Nov 19	*ASCA* GIS	72020000	26.1	3.0±0.1 (GIS2)	(4)
1994 Nov 19			25.7	3.4±0.2 (GIS3)	(4)
1994 Nov 19	*ASCA* SIS	72020000	28.2	9.1±0.3 (SIS0)	(4)
1994 Nov 19			28.2	7.6±0.2 (SIS1)	(4)
1995 May 18	*ASCA* GIS	72020010	10.5	2.5±0.2 (GIS2)	(4)
			10.3	3.3±0.2 (GIS3)	(4)
1995 May 18	*ASCA* SIS	72020010	8.9	8.4±0.4 (SIS0)	(4)
			9.0	6.5±0.3 (SIS1)	(4)
1996 Nov 12	*ROSAT* HRI	RP703893	30	61±2	(4)
1997 Apr 17-18	*SAX* LECS	50172004	21.7	6.9±0.2	(4)
1997 Apr 17-18	*SAX* MECS	50172004	43.2	2.16±0.08	(4)
1997 Apr 14-20	*EUVE* DS/S		97.1	3.8±0.1	(4)

[a](1) Puchnarewicz et al (1995); (2) Fruscione et al. (1996); (3) Fruscione, private communication; (4) this paper; *ASCA* GIS count rates are over 1.0-10 keV; SIS count rates 0.7-10 keV

TABLE 2

FITS TO *ASCA* SPECTRA

Model	intrinsic n_H	α_S or kT (eV)	second BB kT (eV)	α_H	χ^2/dof
72020000 Observation (1994 November)					
One power-law	0.0<0.51	2.04 ± 0.09 1.05×10^{-3}			519/410
Two power-law	0.0<28.6	$3.43^{+2.08}_{-0.63}$ 7.32×10^{-4}		$0.79^{+0.46}_{-0.62}$ 3.07×10^{-4}	363/408
Broken power-law	0.0<7.4	$2.61^{+0.45}_{-0.23}$ 1.07×10^{-3}		$1.27^{+0.20}_{-0.28}$ break 1.51 keV	375/408
Brems+power-law	0.0<16.7	250^{+62}_{-66} 1.68×10^{-2}		1.18 ± 0.25 5.54×10^{-4}	367/408
BB + power-law	0.0<3.7	127^{+17}_{-19} 4.68×10^{-5}		$1.29^{+0.19}_{-0.20}$ 6.25×10^{-4}	371/408
2BB + power-law	0.0<40	122^{+28}_{-62} 6.43×10^{-5}	323^{+157}_{-183} 8.77×10^{-6}	$0.65^{+0.65}_{-1.25}$ 2.57×10^{-4}	362/406
72020010 Observation (1995 May)					
Model	intrinsic n_H	α_S or kT (eV) normalization	normalization	α_H normalization	χ^2/dof
One power-law	0.0<2.2	1.98 ± 0.13 1.04×10^{-3}			151/156
Two power-law	Too poorly constrained - no improvement over one power-law				
Broken power-law	37^{+67}_{-35}	$4.31^{+3.62}_{-1.83}$ 2.54×10^{-3}		$1.79^{+0.62}_{-0.35}$ break 1.40 keV	120/154
Brems+power-law	56^{+56}_{-51}	151^{+117}_{-48} 1.16		$1.82^{+0.60}_{-0.49}$ 1.15×10^{-3}	123/154
BB + power-law	46<99	104^{+58}_{-23} 6.05×10^{-4}		$1.79^{+0.55}_{-0.44}$ 1.11×10^{-3}	124/154
2BB + power-law	Too poorly constrained - no improvement over one blackbody				

[a]Intrinsic n_H is the column density local to the AGN, *in addition* to a Galactic absorbing column density fixed at 1.5×10^{20} cm^{-2}, and corrected for redshift. Limits (given in brackets) are 90%. Power-law indices, α, are defined such that $F_\nu \propto \nu^{-\alpha}$. Bremsstrahlung and blackbody temperatures are given in eV and have been corrected for redshift. Power-law and broken power-law normalizations are in units of photons keV^{-1} cm^{-2} s^{-1} at 1 keV; bremsstrahlung normalization = $3.02\times10^{-15}/(4\pi D^2)\int n_e n_I dV$, where n_e is the electron density in cm^{-3}, n_I is the ion density in cm^{-3} and D is the distance to the source in cm; blackbody normalization = L_{39}/D_{10}^2, where L_{39} is the source luminosity in units of 10^{39} erg s^{-1} and D_{10} is the distance to the source in units of 10 kpc.

TABLE 3

LOG OF BEPPO-SAX OBSERVATIONS

Dates	Exposure		Rate (10^{-2} c/s)	
	LECS	MECS	LECS	MECS
18-19 Apr 1997	21.7ks	43.2ks	6.9 ± 0.2	2.16 ± 0.08

TABLE 4
FITS TO BEPPO-SAX DATA

Model	N_H^a	α_S or kT^b	E_{break}^c or kT^b	α_H	χ^2(dof)
LECS plus MECS 0.1-10 keV					
power-law	1.75±0.35	2.27±0.14	...	...	120.2/92
broken p.l.	2.4±0.5	2.54±0.16	$E_b = 2.3\pm0.5$	$1.13^{+0.29}_{-0.35}$	70.0/90
broken p.l.	1.5(F)	2.24±0.07	$E_b = 2.5\pm0.6$	1.08±0.32	83.2/91
bb+p.l.	$0.5^{+0.5}_{-0.35}$	kT=100±10	...	1.50±0.26	95.1/90
bb+p.l.	1.5(F)	kT=82^{+13}_{-8}	...	1.84±0.25	104.6/91
bb+bb+p.l.	1.5(F)	kT$_1$=55±10	kT$_2$=155^{+26}_{-20}	1.19±0.24	65.7/89
MECS 2-10 keV					
power-law	1.5(F)	1.42±0.26	...	...	31.5/45
LECS 0.1-1.5 keV					
power-law	2.3±0.5	2.45±0.20	...	...	29.9/41

[1] [a] Absorbing column density in units of 10^{20} cm^{-2}; [b] Temperatures in eV. [c] Break energies in keV; (F) frozen parameter. Errors are 90%.